Macromolecules

pubs.acs.org/Macromolecules

Article

Synthesis of Thermoresponsive Diblock Copolymer Nano-Objects via RAFT Aqueous Emulsion Polymerization of Hydroxybutyl Methacrylate

Saul J. Hunter, Nicholas J. W. Penfold, Elizabeth R. Jones, Thomas Zinn, Oleksandr O. Mykhaylyk, and Steven P. Armes*

Cite This: *Macromolecules* 2022, 55, 3051−3062

Read Online

ACCESS | Metrics & More | Article Recommendations | Supporting Information

ABSTRACT: We recently reported that the reversible addition−fragmentation chain transfer (RAFT) aqueous emulsion polymerization of hydroxybutyl methacrylate (HBMA) using a relatively short non-ionic poly(glycerol monomethacrylate) (PGMA) precursor enables convenient preparation of diblock copolymer nano-objects with spherical, worm-like, or vesicular morphologies. We postulated that the relatively high aqueous solubility of HBMA (~25 g dm^{-3} at 50 °C) was likely to be a key parameter for overcoming the problem of kinetically trapped spheres that is observed for many RAFT aqueous emulsion polymerization formulations. In this study, we revisit the RAFT aqueous emulsion polymerization of HBMA using a poly(ethylene glycol) (PEG) precursor as a steric stabilizer block. Remarkably, the resulting PEG_{45}−$PHBMA_{20}$ diblock copolymer nanoparticles exhibit thermoreversible morphological transitions in aqueous solution. More specifically, transmission electron microscopy and small-angle X-ray scattering studies confirmed that spheres are formed at 25 °C, worms at 58 °C, and vesicles at 65 °C. This is the first time that such behavior has been reported for nano-objects prepared by RAFT aqueous emulsion polymerization. Moreover, variable temperature dynamic light scattering and oscillatory rheology studies confirmed that these transitions are highly reversible at 0.1 and 10% w/w, respectively. Variable temperature ^{1}H NMR studies indicated that (i) the PEG stabilizer block undergoes dehydration on heating and (ii) the apparent degree of hydration of the hydrophobic PHBMA block increases on heating from 25 to 65 °C. This suggests that the change in copolymer morphology is best explained in terms of a uniform plasticization mechanism.

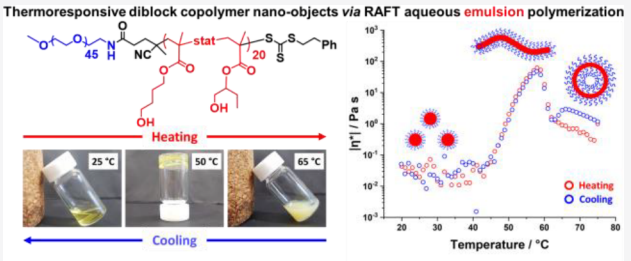

INTRODUCTION

It is well-known that polymerization-induced self-assembly (PISA) enables the convenient and efficient preparation of a wide range of diblock copolymer nano-objects in the form of concentrated dispersions.[1−26] In the case of aqueous PISA formulations, if the vinyl monomer used to grow the hydrophobic second block is water-miscible, this corresponds to an aqueous dispersion polymerization.[3,17,21,27−35] On the other hand, if the monomer is water-immiscible—which is much more common—this corresponds to an aqueous emulsion polymerization.[36−38] In the PISA literature, there has been substantial interest in the rational design of aqueous dispersions of thermoresponsive shape-shifting diblock copolymer nano-objects over the past decade.[17,39−46] In practice, such nano-objects are invariably prepared via RAFT aqueous dispersion polymerization.[3,47−50] This is because water-miscible vinyl monomers such as 2-hydroxypropyl methacrylate (HPMA),[27,51−54] 4-hydroxybutyl acrylate (HBA),[35,46,55] *N*-isopropylacrylamide,[17,42] or 2-methoxyethyl acrylate[29,31] produce homopolymers that are only weakly hydrophobic. In particular, their degree of (partial) hydration is temperature-dependent, which affects the relative volume fraction of such hydrophobic blocks.[39,46] This induces a subtle change in the fractional packing parameter *P*,[56,57] which is sufficient to drive various morphological transitions for the corresponding diblock copolymer nano-objects when adjusting the solution temperature.[39,45,46,54,55,62−66] For example, Ratcliffe and co-workers reported that a single poly(2-hydroxypropyl methacrylamide)−poly(2-hydroxypropyl methacrylate) ($PHPMAC_{41}$−$PHPMA_{180}$) diblock copolymer formed spheres at 4 °C, worms at 22 °C, and vesicles at 50 °C.[45]

Recently, we have reported five examples of HBA-based thermoresponsive diblock copolymers of fixed composition that can form spheres, worms, or vesicles in aqueous solution simply by adjusting the solution temperature.[46,58−61] Initially, Byard et al. prepared thermoresponsive poly(*N*,*N*′-dimethyl-

Received: February 22, 2022
Revised: April 1, 2022
Published: April 17, 2022

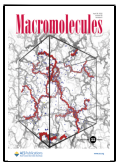

https://doi.org/10.1021/acs.macromol.2c00379
Macromolecules 2022, 55, 3051−3062

acrylamide)−poly(4-hydroxybutyl acrylate) ($PDMAC_{56}$−$PHBA_{218-269}$) worms via RAFT aqueous dispersion polymerization of HBA at 20% w/w solids.[62] Spheres were formed on cooling to 3 °C, whereas heating to 50 °C led to the formation of vesicles. Variable temperature ^{1}H NMR studies indicated that the weakly hydrophobic HBA repeat units became *more* hydrated at elevated temperature. This is in striking contrast to the behavior observed for PHPMA-based diblock copolymers, where the HPMA repeat units become *less* hydrated on heating.[39,53,61,63−67] Such contrasting behavior is rather counterintuitive given that HPMA and HBA are structural isomers. Unfortunately, the relatively low T_g of the PHBA block led to film formation, which prevented the determination of copolymer morphologies via TEM.[62] Subsequently, Byard et al. addressed this technical issue by statistically copolymerizing HBA with a cross-linkable diacetone acrylamide (DAAM) comonomer.[46] Covalent stabilization using adipic acid dihydrazide prevented film formation and hence enabled TEM studies. However, the presence of 20 mol % DAAM comonomer reduced the thermoresponsive behavior exhibited by the HBA-rich structure-directing block. Recently, this limitation was overcome by Deane et al., who prepared a series of poly(2-(*N*-(acryloyloxy)ethylpyrrolidone)−poly(4-hydroxybutyl acrylate) ($PNAEP_{85}$−$PHBA_x$) diblock copolymer nano-objects. In this case, glutaraldehyde was reacted with the pendent hydroxyl groups on the PHBA block to covalently stabilize the nanoparticles. This approach enabled high-quality TEM images of $PNAEP_{85}$−$PHBA_{295}$ nano-objects to be obtained without incorporating a second cross-linkable comonomer (e.g. DAAM) within the structure-directing block. This enabled direct evaluation of the thermoresponsive behavior of purely PHBA-based nano-objects. More specifically, raising the temperature drives morphological transitions from spheres (5 °C) to worms (23 °C) to vesicles (31 °C) and finally lamellae (41 °C). Moreover, such transitions proved to be fully reversible on cooling.

In striking contrast, the RAFT aqueous emulsion polymerization of relatively hydrophobic vinyl monomers such as styrene,[68−74] methyl methacrylate,[75−77] benzyl methacrylate,[78,79] *n*-butyl acrylate,[73,75,80] phenyl acrylate,[81] vinyl acetate,[82−85] or 2,2,2-trifluoroethyl methacrylate[86−89] invariably leads to the formation of block copolymer nano-objects that do *not* exhibit any thermoresponsive behavior. Moreover, such formulations often lead solely to kinetically trapped spheres, although there are a few well-known counter-examples to this morphological limitation.[20,69,70,90−94] Recently, Armes and co-workers explored the RAFT aqueous emulsion polymerization of vinyl monomers such as glycidyl methacrylate,[95−97] 2-methoxyethyl methacrylate,[98] or hydroxybutyl methacrylate (HBMA)[99,100] which exhibit moderate aqueous solubilities (e.g., 15−20 g dm^{-3}) at 20 °C. This has provided access to well-defined worms and vesicles, as well as spheres. However, such nano-objects typically do not exhibit thermoresponsive behavior.

Herein we report the RAFT aqueous emulsion polymerization of HBMA using a trithiocarbonate-capped PEG precursor. We demonstrate that this system provides the first example of thermoresponsive diblock copolymer nano-objects to be prepared by using such an aqueous PISA formulation. Moreover, PEG−PHBMA spheres, worms or vesicles can be formed reversibly in aqueous solution simply by varying the solution temperature.

RESULTS AND DISCUSSION

PEG_{45}−$PHBMA_{20}$ diblock copolymer nano-objects were synthesized by RAFT aqueous emulsion polymerization of HBMA using a previously reported trithiocarbonate-based PEG_{45}-TTC precursor[64] (see Figure 1). These syntheses were performed using an azo-based VA-044 initiator at 50 °C and a PEG_{45}-TTC/VA-044 molar ratio of 5.0 while targeting 10% w/w solids.

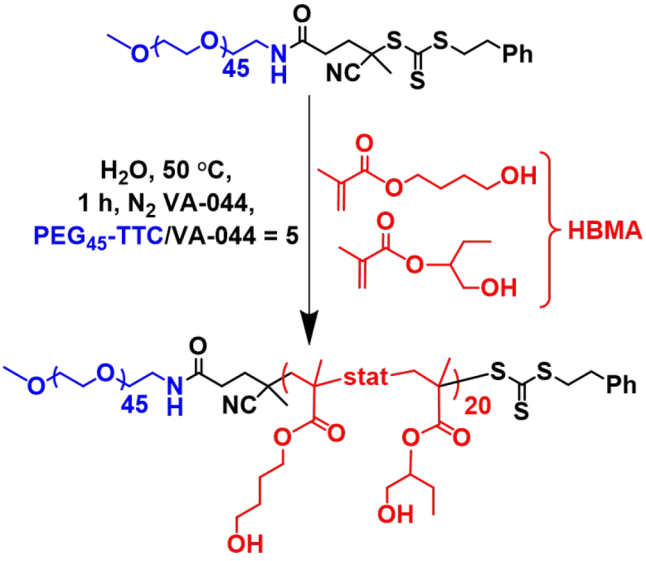

Figure 1. RAFT aqueous emulsion polymerization of HBMA at 50 °C using a trithiocarbonate-based PEG_{45}-TTC precursor and a PEG_{45}-TTC/VA-044 molar ratio of 5.0 while targeting 10% w/w solids (N.B. HBMA monomer comprises a 1:1 mixture of the 2- and 4-isomers; the chemical structure of both isomers is indicated on the reaction arrow).

^{1}H NMR spectroscopy studies of PEG_{45}−$PHBMA_{20}$ in CD_3OD (which leads to molecular dissolution of the initial nano-objects) confirmed that a HBMA conversion of more than 99% was achieved within 1 h at 50 °C (see Figure S1). DMF GPC curves obtained for the PEG_{45}−$PHBMA_{20}$ diblock copolymer using either a refractive index or a UV detector tuned to the absorption wavelength of the trithiocarbonate RAFT chain-end (λ = 305 nm) are shown in Figure S2. In each case, these GPC curves are shifted relative to that of the corresponding PEG_{45}-TTC precursor, which indicates a relatively high blocking efficiency and minimal homopolymer contamination. Moreover, a relatively narrow unimodal molecular weight distribution was obtained (M_w/M_n = 1.11), which is consistent with those previously reported for $PGMA_{41}$−$PHBMA$ diblock copolymers.[100] Targeting higher PHBMA DPs led to a systematic increase in M_w/M_n because of the presence of dimethacrylate impurities in the HBMA monomer, which inevitably causes chain branching.[22,45,101] Visual inspection confirmed that the final 10% w/w aqueous dispersion of PEG_{45}-$PHBMA_{20}$ nano-objects was a transparent free-flowing fluid at 20 °C. This was not unexpected because the relatively short PHBMA DP should favor the formation of spheres. Indeed, TEM studies confirmed that these nano-objects possessed a spherical morphology (see Figure 3a) while DLS studies indicated a *z*-average diameter of 17 nm (PDI = 0.09).

https://doi.org/10.1021/acs.macromol.2c00379
Macromolecules 2022, 55, 3051−3062

On quenching the HBMA polymerization at 50 °C, the 10% w/w PEG_{45}–$PHBMA_{20}$ dispersion was highly viscous. However, a free-flowing dispersion was obtained after cooling to 20 °C. This physical transformation suggested that these PEG_{45}–$PHBMA_{20}$ nano-objects were likely to possess thermoresponsive character. To explore this hypothesis, the 10% w/w dispersion was immersed in an oil bath and heated to 25, 55, or 65 °C for 10 min while recording digital photographs (see Figure 2). On heating to 55 °C, a relatively transparent free-standing gel was obtained. On further heating to 65 °C, degelation occurred to produce a free-flowing turbid dispersion. Such transformations proved to be fully reversible as judged by visual inspection.

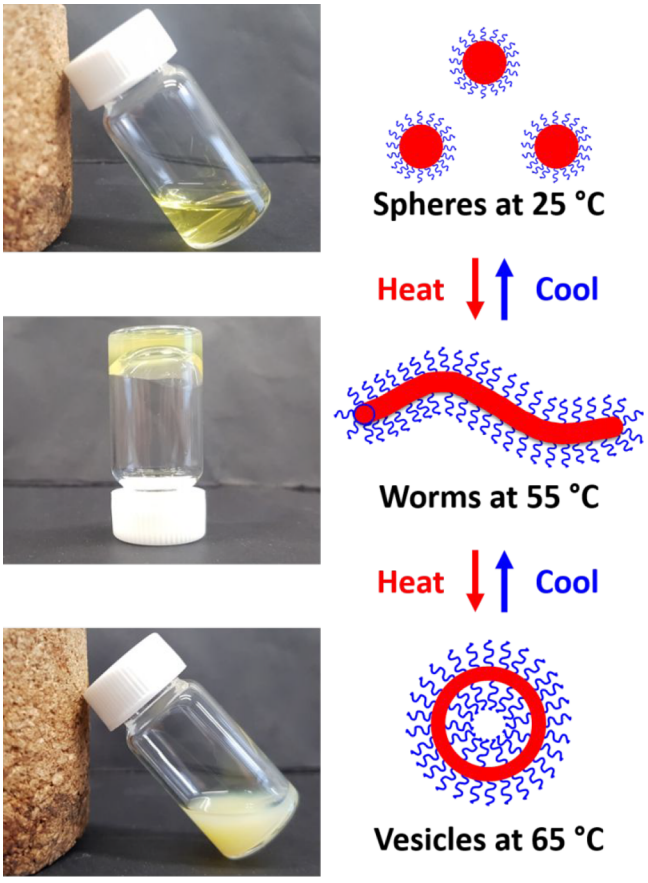

Figure 2. Digital images (left) illustrating the physical appearance of a 10% w/w PEG_{45}–$PHBMA_{20}$ aqueous dispersion: (top) at 25 °C, (middle) on heating to 55 °C for 10 min, and (bottom) on heating to 65 °C for 10 min. Schematic representation (right) of the likely thermoreversible morphological transitions exhibited by these diblock copolymer nano-objects. N.B. The observed yellow color arises from the trithiocarbonate chain-ends.

There are numerous examples of thermoresponsive diblock copolymer nano-objects in the PISA literature.[33,39,44−46,53−55,59,63,66,102−110] To examine whether PEG_{45}–$PHBMA_{20}$ nano-objects also exhibit thermally-induced changes in morphology, TEM studies were performed for 0.1% w/w aqueous dispersions after drying at 25, 58, 65, or 75 °C. Unlike previously reported temperature-dependent studies on PHBA-based diblock copolymers,[46,59,111] the PEG_{45}–$PHBMA_{20}$ nano-objects studied herein do not require covalent stabilization prior to their visualization by TEM. This is because the methacrylic block has a sufficiently high T_g to prevent film formation during TEM grid preparation. Hence the PEG_{45}–$PHBMA_{20}$ nano-objects can be analyzed directly.[55] TEM studies confirmed that PEG_{45}–$PHBMA_{20}$ undergoes morphological transitions that resemble those reported for PHBA-based diblock copolymers.[112] More specifically, PEG_{45}–$PHBMA_{20}$ forms spheres at 25 °C, anisotropic worms at 55 °C, vesicles at 65 °C, and lamellae at 75 °C (see Figure 3). Such thermoresponsive behavior is perhaps surprising given the significantly greater hydrophobic character of HBMA monomer (aqueous solubility ~30 g dm^{-3} at 20 °C) compared to that of HBA (which is miscible with water in all proportions at 20 °C). One subtle difference between PHBA- and PHBMA-based diblock copolymer nano-objects is the preferred morphology at ambient temperature. For example, Deane et al. reported that $PNAEP_{85}$–$PHBA_{295}$ worms undergo a worm-to-sphere on cooling to 5 °C, whereas on heating to 34 °C they undergo a worm-to-vesicle transition. In contrast, PEG_{45}–$PHBMA_{20}$ forms spheres at ambient temperature, which undergo a sphere-to-worm transition at 55 °C followed by a worm-to-vesicle transition on heating to 70 °C. In summary, these two diblock copolymers undergo the same thermal transitions, but higher onset temperatures are required to produce worms and vesicles in the case of PEG_{45}–$PHBMA_{20}$.

DLS was used to determine the sphere-equivalent *z*-average diameter for a 0.10% w/w aqueous dispersion of PEG_{45}–$PHBMA_{20}$ nano-objects during a thermal cycle from 20 °C to 75 °C to 20 °C (Figure 4a). Initially, this dispersion comprised relatively small spheres (17 nm diameter, PDI = 0.09). At 44 °C, the *z*-average diameter and DLS polydispersity both begin to increase rapidly, which is characteristic of a sphere-to-worm transition.[46,113] A dramatic increase in size and a concomitant reduction in DLS polydispersity occur above 60 °C, suggesting the formation of relatively small, well-defined vesicles (*z*-average diameter = 117 nm, DLS polydispersity = 0.05). Comparable *z*-average diameters were recorded during the cooling cycle, indicating remarkably good thermoreversibility at this relatively low copolymer concentration.

Oscillatory rheological studies conducted on a 10% w/w aqueous dispersion of PEG_{45}–$PHBMA_{20}$ nano-objects confirmed that a low-viscosity fluid was obtained between 20 and 50 °C (see Figure 4b). Further heating of this dispersion produced a soft, highly transparent, free-standing gel (Figure 2). More specifically, the storage modulus (G') exceeds the loss modulus (G'') at around 52 °C (see Figure S3), and a maximum $|\eta^*|$ of 62 Pa s (which corresponds to a maximum G' value of around 45 Pa) is attained at 58 °C (see Figure 4b). According to Lovett and co-workers, such macroscopic gelation is the result of multiple interworm contacts, which leads to the formation of a 3D percolating network.[104] It is perhaps noteworthy that this PEG_{45}–$PHBMA_{20}$ worm gel is somewhat weaker than the PEG_{113}–$PHPMA_{220}$ worm gel reported by Warren et al.[28] (G' = 65 Pa at 11 °C). However, direct comparison between the PEG_{45}–$PHBMA_{20}$ worms reported herein and the previously reported PEG_{113}–$PHPMA_{220}$ worms is somewhat problematic given the different PEG stabilizer block DPs. Furthermore, a much lower PHBMA DP is required to access the worm phase because this core-forming block is significantly more hydrophobic than either PHBA[58,60,61] or PHPMA.[27,65] Heating the PEG_{45}–$PHBMA_{20}$ dispersion above 58 °C resulted in a substantial reduction in viscosity, suggesting a worm-to-vesicle transition.[46,114] Heating to 75 °C led to a second, smaller increase in viscosity, which

https://doi.org/10.1021/acs.macromol.2c00379
Macromolecules 2022, 55, 3051−3062

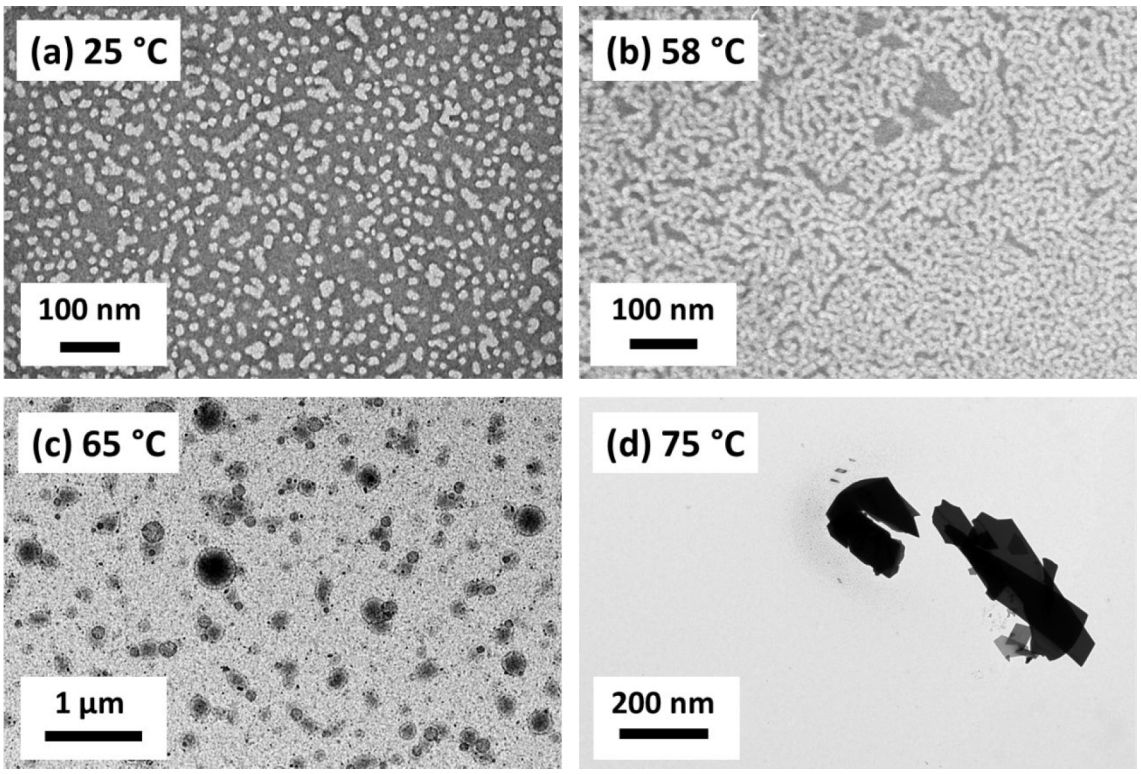

Figure 3. Representative TEM images obtained for a 0.1% w/w aqueous dispersion of PEG_{45}−$PHBMA_{20}$ nano-objects at (a) 25 °C (spheres) and after heating for 30 min to (b) 58 °C (worms), (c) 65 °C (vesicles), or (d) 75 °C (lamellae).

corresponds to the formation of lamellae (see Figure 3d).[46] These thermal transitions proved to be remarkably reversible, with relatively little hysteresis being observed at heating/cooling rates of 1 °C min^{-1}. Exceptionally, hysteresis is observed for the vesicle-to-lamellae transition: very similar observations were reported by both Wilson[62] and Deane and co-workers.[58] This strongly suggests that such hysteresis is most likely characteristic of the precise mechanism for the structural transformation between vesicles and lamellae. Such observations clearly warrant further studies.

Shear-induced polarized light imaging (SIPLI) studies were conducted from 20 to 75 °C to provide further evidence for the thermally induced changes in copolymer morphology. According to Mykhaylyk and co-workers, this optorheological technique enables the alignment of anisotropic nano-objects such as block copolymer worms and lamellae to be visualized at a certain critical rate of applied shear.[115−117] At 20 °C, only a uniform dark image was observed for the 10% w/w aqueous dispersion of PEG_{45}−$PHBMA_{20}$ nano-objects at an applied maximum shear rate of 1.0 s^{-1} (see Figure S4). This lack of birefringence indicates the presence of isotropic spheres. At 60 °C, a distinctive Maltese cross is observed, which is characteristic of anisotropic nano-objects.[65,118] This feature is the result of birefringence produced by *in situ* shear alignment of the worms.[46] It disappears above 60 °C, which is consistent with a worm-to-vesicle transition, while a new (albeit weaker) Maltese cross is observed at 70 °C. The latter feature indicates the presence of anisotropic lamellae possessing either a perpendicular or a transverse orientation.[46] However, the onset temperature required to produce lamellae is lower than the 75 °C indicated by the oscillatory rheology data shown in Figure 4b. This is because the applied (continuous) shear used for the SIPLI experiment produces a greater strain, which promotes the transition from vesicles to lamellae.[46]

Small-angle X-ray scattering (SAXS) studies were conducted on a 1.0% w/w aqueous dispersion of PEG_{45}−$PHBMA_{20}$ nano-objects as a function of temperature. Figure 5 shows selected SAXS patterns recorded at 20, 55, 65, and 70 °C; three of these patterns could be satisfactorily fitted (see solid white lines) using well-known scattering models (see the Supporting Information).[104,105] In each case, the dimensions calculated from these SAXS fits were consistent with those determined by DLS and TEM (see Table 1). SAXS analysis of the spheres formed at 20 °C indicated a volume-average core diameter of 13.8 nm, which is consistent with the overall hydrodynamic *z*-average diameter of 17.6 nm indicated by DLS. For the anisotropic worms formed at 55 °C, the volume-average cross-sectional core diameter T_w was calculated to be 11.5 nm, which is in reasonably good agreement with the number-average worm width of 11.2 nm estimated by TEM. The gradual increase in the apparent sphere-equivalent DLS diameter at around 40 °C (see Figure 4a) indicates that the formation of these PEG_{45}−$PHBMA_{20}$ worms involves stochastic 1D fusion of multiple spheres, which has been observed for other PISA formulations.[22,65,109,113] In principle, a modest reduction in cross-sectional diameter is expected when cylindrical worms are formed via fusion of multiple spheres (see Figure S5).[54] Under such circumstances, the worm core diameter divided by the sphere core diameter should be equal to the square root of 2/3, or ≈0.82. This is consistent with the worm/sphere diameter ratio of 11.5 ÷ 13.8 = 0.83 calculated by SAXS analysis of the corresponding PEG_{45}−$PHBMA_{20}$ nano-objects.

At 65 °C, SAXS analysis indicated that relatively small vesicles were formed with a volume-average diameter of 119 ± 46 nm, which is consistent with the *z*-average diameter of 120

https://doi.org/10.1021/acs.macromol.2c00379
Macromolecules 2022, 55, 3051−3062

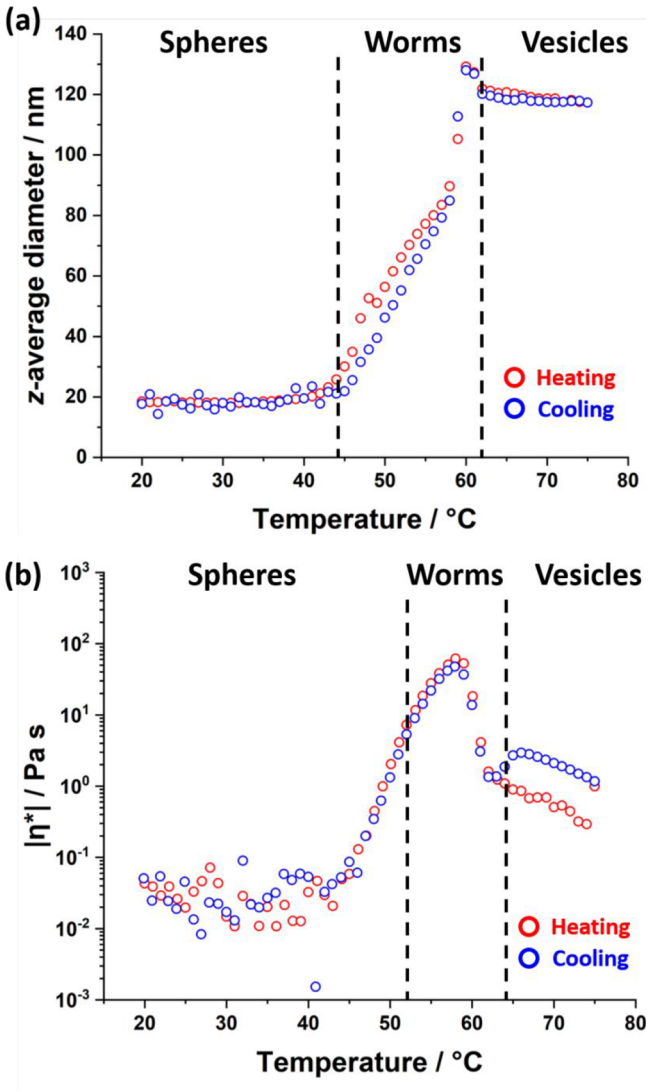

Figure 4. (a) Apparent sphere-equivalent *z*-average diameter determined by DLS as a function of temperature for a 0.1% w/w dispersion of PEG_{45}–$PHBMA_{20}$ nano-objects. The red data were recorded on heating from 20 to 75 °C while the blue data were recorded on cooling from 75 to 20 °C. The dispersion was equilibrated at each temperature for 5 min prior to DLS measurements. The black dashed lines indicate the likely phase boundaries for the three copolymer morphologies (spheres, worms, and vesicles). (b) Complex viscosity $|\eta^*|$ as a function of temperature for a 20 °C to 75 °C to 20 °C thermal cycle obtained for a 10% w/w aqueous dispersion of PEG_{45}–$PHBMA_{20}$ nano-objects at an applied strain of 1.0% and an angular frequency of 1.0 rad s^{-1}. This dispersion was equilibrated at 20 °C for 10 min prior to a thermal cycle conducted at a heating/cooling rate of 1 °C min^{-1}. The black dashed lines indicate the sol–gel and gel–sol transitions that occur during this cycle, as indicated from the relationship between G' and G''.

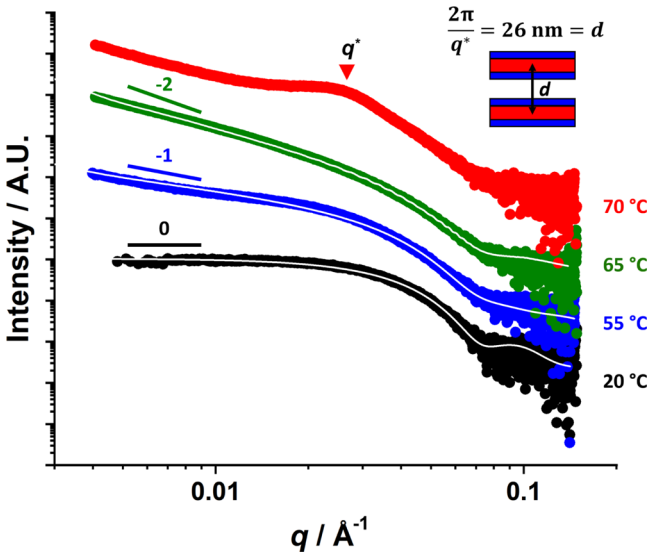

Figure 5. Representative double-logarithmic $I(q)$ vs q SAXS patterns recorded for a 1.0% w/w aqueous dispersion of thermoresponsive PEG_{45}–$PHBMA_{20}$ nano-objects at 20 °C (black), 55 °C (blue), 65 °C (green), and 70 °C (red). The solid white line within each of the first three patterns indicates the data fits obtained by using appropriate scattering models (see the Supporting Information for further details).[119,120] The characteristic low q gradients expected for spheres, worms, and vesicles (0, −1 and −2, respectively) are included as a guide for the eye. No data fit could be obtained for the red pattern recorded at 70 °C for the lamellae. However, the mean distance, d, between stacked lamellae was calculated from the structure peak labeled q^* by using the equation shown in the inset.

± 27 nm reported by DLS. On the basis of TEM analysis, the larger standard deviation indicated by SAXS appears to be more reliable than that suggested by DLS. The mean membrane thickness was 5.5 nm, which indicates significant interdigitation of the structure-directing hydrophobic chains;[121] similar observations were reported for thermoresponsive PHBA-based nano-objects.[46,58,59] Finally, a relatively broad structure peak (q^* = 0.024 Å) becomes visible at 75 °C, which suggests the presence of stacked lamellar sheets.[46] This is consistent with TEM studies of the nano-objects that are formed at 75 °C (see Figure 5). For this SAXS pattern, the relation $d = 2\pi/q^*$ was used to estimate a mean intersheet separation distance of 26 nm.[46]

A series of SAXS patterns recorded for a 1.0% w/w aqueous dispersion of PEG_{45}–$PHBMA_{20}$ nano-objects on heating from 20 to 70 °C at 1 °C min^{-1} (Figure 6a) clearly demonstrate morphological transformation from spheres to worms to vesicles and, finally, to lamellae. In each case, the gradient of the scattering intensity in the low q region is characteristic of the predominant copolymer morphology, as shown in Figure 6b.[122] The low q gradient is close to zero from 20 to 40 °C, suggesting the presence of spheres over this temperature range. At around 50 °C, the low q gradient tends toward −1, indicating the formation of highly anisotropic worms. At around 65 °C, the low q gradient is close to −2, which is characteristic of bilayer (or vesicle) formation. At 70 °C, the broad structure factor observed at around 0.024 Å indicates the presence of stacked lamellae sheets.[46] Clearly, these SAXS data are consistent with the copolymer morphologies observed by TEM and rheology.

Moreover, SAXS analysis also indicated that the water volume fraction associated with the core-forming PHBMA block, x_{sol}, remained constant at around 0.001 on heating from 20 to 50 °C (see Table 1). However, x_{sol} increased significantly to 0.18 on heating to 65 °C. A subtle increase in the (partial) degree of hydration of the core-forming block has been shown to be responsible for thermally-induced morphological transitions exhibited by diblock copolymer nano-objects prepared via RAFT aqueous dispersion polymerization.[39,46] For example, Deane et al. used SAXS to calculate that x_{sol} for

https://doi.org/10.1021/acs.macromol.2c00379
Macromolecules 2022, 55, 3051−3062

Table 1. Summary of the Various Structural Parameters Calculated from SAXS Analysis of a 1.0% w/w Aqueous Dispersion of PEG_{45}-$PHBMA_{20}$ Nano-Objects at 20, 55 or 65 °C[a]

temp/°C	morphology	D_s/nm[b]	D_w/nm[c]	D_v/nm[d]	T_m/nm	x_{sol}
20	spheres	13.8 ± 2.2				0.001
55	worms		11.5 ± 2.0			0.001
65	vesicles			119 ± 46	10.7 ± 0.6	0.18

[a]D_s is the volume-average sphere diameter, D_w is the volume-average worm cross-sectional diameter, D_v is the overall volume-average diameter of the vesicles, T_m is the mean vesicle membrane thickness, and x_{sol} is the volume fraction of water within the hydrophobic PHBMA core/membrane. [b]Using a spherical micelle model,[120] D_s was calculated via $D_s = 2R_s + 4R_g$, where R_s is the mean spherical micelle core radius and R_g represents the radius of gyration of the PEG_{45} stabilizer block. [c]Using a worm-like model,[120] D_w was calculated via $D_w = 2R_w + 4R_g$, where R_w is the mean volume-average cross-sectional worm radius. [d]Using a vesicle model,[120] D_v was calculated via $D_v = 2R_m + T_m + 4R_g$, where R_m is the mean volume-average radius from the center of the vesicle to the center of the membrane.

the PHBA core-forming block increased from 0.10 to 0.68 on heating PEG_{113}−$PHBA_{260}$ nano-objects from 10 to 50 °C.[59] These x_{sol} values are consistent with those calculated for PEG_{45}−$PHBMA_{20}$ nano-objects in this study, particularly given that PHBMA is significantly more hydrophobic than PHBA.[35] Thus, PHBMA is expected to become somewhat less hydrated than PHBA on heating. Nevertheless, the increase in (partial) hydration of the former block is clearly sufficient to cause PEG_{45}−$PHBMA_{20}$ nano-objects to undergo morphological transitions at elevated temperatures.

It is well-known that thermoresponsive PHPMA-based worms undergo a worm-to-sphere transition on *cooling* because of (partial) hydration of the HPMA repeat units that lie close to the block junction.[39,45] This LCST-like behavior has been described as *surface* plasticization.[3] In contrast, PHBA-based nano-objects exhibit UCST-like behavior: in this case, an increase in (partial) hydration of the hydrophobic block occurs on *heating*, which corresponds to *uniform* plasticization.[46,109] Accordingly, variable temperature ^{1}H NMR spectroscopy studies were conducted to elucidate the molecular mechanism responsible for the thermoresponsive behavior observed for PEG_{45}−$PHBMA_{20}$ nano-objects.

Variable temperature ^{1}H NMR spectroscopy studies were conducted between 20 and 75 °C on a 10% w/w aqueous dispersion of PEG_{45}−$PHBMA_{20}$ nano-objects prepared in D_2O. ^{1}H NMR spectra normalized relative to an external standard (pyridine) are shown in Figure 7, along with two sets of partial spectra highlighting regions of particular interest. ^{1}H NMR signals assigned to the PEG_{45} stabilizer chains become broader and less prominent at higher temperature, indicating a progressively lower degree of hydration for this water-soluble block. This is consistent with literature data for aqueous solutions of PEO homopolymers, which undergo phase separation at elevated temperatures.[123−125] In contrast, ^{1}H NMR signals assigned to the oxymethylene (*m*) and methacrylic backbone protons (*b*, *h*, *j*, *k*) of the structure-directing PHBMA chains at around 3.7 and 1.0 ppm respectively, become progressively more intense on heating (see Figures 7c and 7d). This indicates that this weakly hydrophobic block becomes more hydrated, particularly at higher temperatures. These observations are consistent with the SAXS studies, which indicate a significant increase in the solvent volume fraction, x_{sol}, associated with the PHBMA chains between 55 and 65 °C (see Table 1). However, it is rather surprising that such spectral changes only become apparent above 65 °C, whereas the sphere-to-worm and worm-to-vesicle transitions occur at significantly lower temperatures. Unfortunately, such spectral changes cannot be easily quantified because of overlap between the PEG and PHBMA signals at 3.7−3.8 ppm. Nevertheless, these ^{1}H NMR studies indicate that a significant reduction in the degree of hydration of the PEG stabilizer chains occurs on heating. Indeed, the spectra shown in Figure 7 suggest that the sphere-to-worm and worm-to-vesicle transitions appear to be mainly driven by (partial) dehydration of the PEG stabilizer block, whereas the vesicle-to-lamellae transition is driven by an increase in the degree of (partial) hydration of the PHBMA block. We now seek to rationalize this hypothesis in terms of the fractional packing parameter, *P*, originally introduced by Israelachvili and co-workers to account for the micellization of small-molecule surfactants[56] and more recently applied to the self-assembly of amphiphilic diblock copolymers.[57]

The packing parameter *P* is given by the following equation:

$$P = \frac{V}{a_0 l_c} \quad (1)$$

For the PEG_{45}−$PHBMA_{20}$ diblock copolymer, *V* is the volume occupied by the hydrophobic PHBMA block, a_0 is the optimal area occupied by the head-group (in this case, the PEG stabilizer), and l_c is the length of the PHBMA block.

It is well-known that aqueous solutions of PEG homopolymer exhibit LCST-type behavior.[126−130] In principle, partial dehydration of the PEG stabilizer chains at higher temperatures should lead to an increase in the packing parameter *P*, which would account for the observed sphere-to-worm and worm-to-vesicle transitions (spheres are formed when $P < 1/3$ and worms are favored when $1/3 < P < 1/2$). However, variable temperature SAXS and ^{1}H NMR studies indicate that there is also a subtle increase in the (partial) degree of hydration of the structure-directing PHBMA block between 65 and 75 °C. If *surface* plasticization of the PHBMA block occurred at 75 °C, the HBMA residues near the block junction would become hydrated and *V* would decrease, which would lead to a concomitant *reduction* in *P*. However, this is not consistent with the experimental observations because this indicates that a vesicle-to-worm transition should occur. In contrast, *uniform* plasticization of the PHBMA block increases *V* and hence leads to the desired increase in *P*. Hence, *uniform* plasticization most likely accounts for the vesicle-to-lamellae transition exhibited by the PEG_{45}−$PHBMA_{20}$ diblock copolymer, as depicted in Figure 8. Similar UCST-like behavior has been reported for PHBA-based diblock copolymers.[46,58] It is perhaps also worth noting that the likely further (partial) dehydration of the PEG stabilizer chains would also lead to an increase in the relative volume fraction of the hydrophobic PHBMA block.

As far as we are aware, this study constitutes the first example of amphiphilic diblock copolymer nano-objects

https://doi.org/10.1021/acs.macromol.2c00379
Macromolecules 2022, 55, 3051−3062

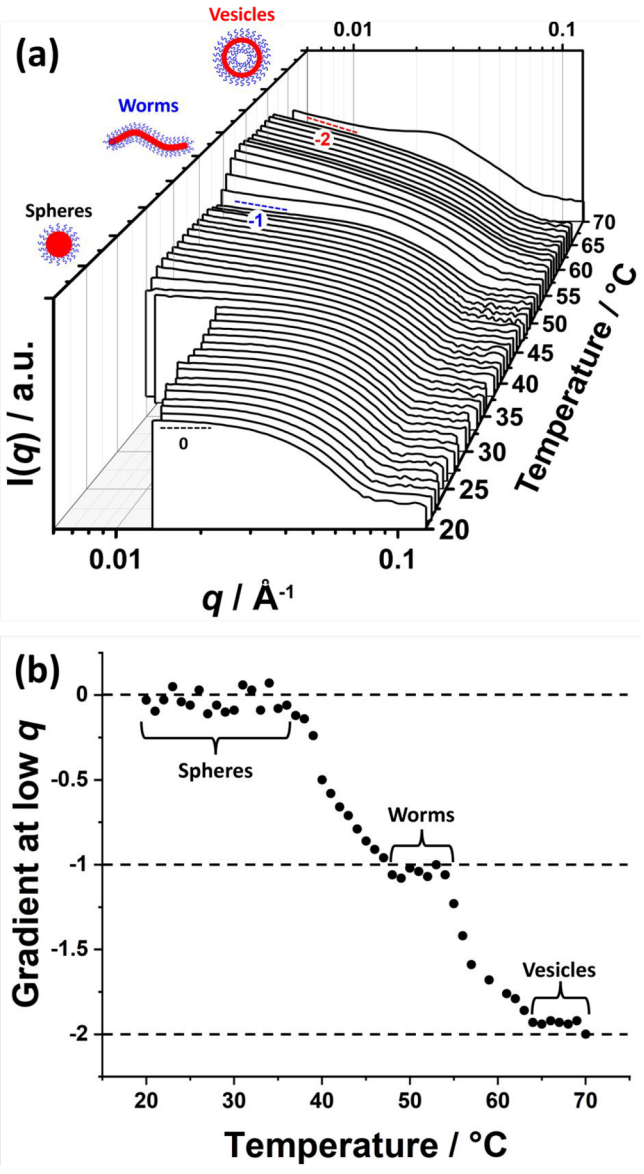

Figure 6. (a) SAXS patterns recorded between 20 and 70 °C for a 1.0% w/w aqueous dispersion of thermoresponsive PEG_{45}–$PHBMA_{20}$ nano-objects prepared at 10% w/w solids with a heating rate of 1 °C min^{-1}. The characteristic low q gradients expected for spheres, worms, and vesicles (0, −1, and −2, respectively) are included as a guide for the eye (see the black, bluedashed lines indicate the characteristic and red dashed lines). In addition, there is a prominent structure factor in the final SAXS pattern recorded at 70 °C, which indicates interlamellar stacking. (b) Variation in the low q gradient ($0.006 \leq q \leq 0.015$ $Å^{-1}$) for the SAXS patterns shown in (a) as a function of temperature. The horizontal dashed lines indicate the characteristic low q gradients (0, −1, and −2) which indicate the presence of spheres, worms and vesicles, respectively.

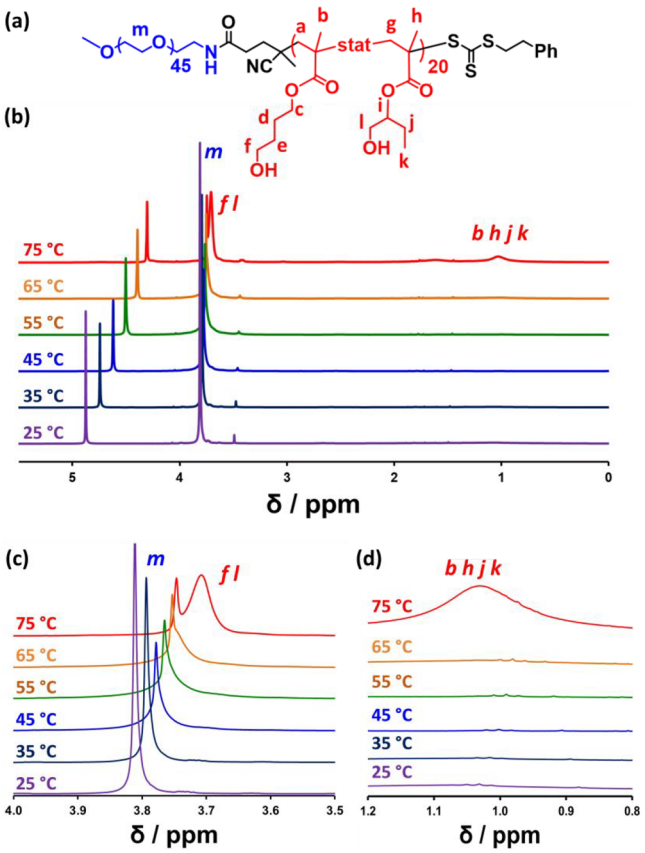

Figure 7. Variable temperature ^1H NMR studies of thermoresponsive PEG_{45}–$PHBMA_{20}$ diblock copolymer nano-objects. (a) Chemical structure of the PEG_{45}–$PHBMA_{20}$ diblock copolymer showing the two types of HBMA repeat units. (b) Normalized (relative to a pyridine external standard) ^1H NMR spectra recorded from 25 to 75 °C for a 10% w/w aqueous dispersion of PEG_{45}–$PHBMA_{20}$ nano-objects prepared in D_2O. (c) Overlaid partial spectra recorded between 25 °C (purple) and 75 °C (red) for the oxymethylene protons (m) assigned to the PEG_{45} chains. This signal clearly becomes broader and weaker at higher temperatures, suggesting that this steric stabilizer block becomes less hydrated. (d) Overlaid partial spectra recorded between 25 °C (purple) and 75 °C (red). The signal at around 0.95−1.15 ppm assigned to the methacrylic backbone protons (b, h, j, k) of the PHBMA chains becomes visible at higher temperatures, indicating partial solvation of this block. In addition, a broad signal (f, l) at around 3.70−3.75 ppm is observed as a shoulder on the oxymethylene proton signal (m) assigned to the PEG_{45} chains at and above 65 °C, see panel (c). This new signal is assigned to the HO−CH_2− protons on the HBMA repeat units.

prepared via RAFT aqueous emulsion polymerization that display thermoresponsive behavior. However, HBMA has a relatively high aqueous solubility of 25 g dm^{-3} at 50 °C. Thus, when targeting PEG_{45}–$PHBMA_{20}$ nano-objects at 10% w/w solids, a significant minority (~42%) of this monomer is soluble within the aqueous continuous phase at this reaction temperature. Arguably, such aqueous PISA formulations lie somewhere between an aqueous emulsion polymerization and an aqueous dispersion polymerization. To increase the proportion of water-immiscible HBMA monomer, the synthesis of PEG_{45}–$PHBMA_{20}$ nano-objects was repeated targeting 30% w/w solids. Under such conditions, approximately 86% of the HBMA is water-immiscible at 50 °C. Gratifyingly, the resulting PEG_{45}–$PHBMA_{20}$ spheres displayed similar thermoreversible behavior as those prepared at 10% w/w solids. More specifically, variable temperature SAXS experiments confirmed that heating such nanoparticles from 20 to 55 °C led to the formation of worms. Moreover, further heating to 65 °C led to the formation of vesicles (see Figure 9).

CONCLUSIONS

Amphiphilic PEG_{45}–$PHBMA_{20}$ diblock copolymer nano-objects have been prepared by chain-extending a water-soluble PEG_{45}-TTC precursor via RAFT aqueous emulsion polymerization of HBMA at 50 °C. More than 99% conversion was

https://doi.org/10.1021/acs.macromol.2c00379
Macromolecules 2022, 55, 3051−3062

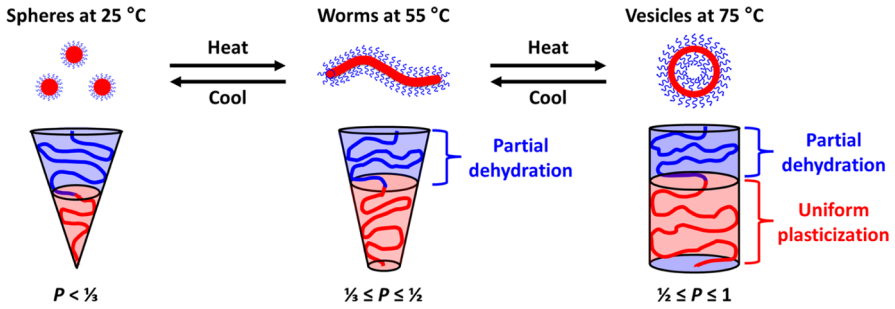

Figure 8. Schematic representation of the partial dehydration of the blue PEG stabilizer block at 55 °C and the uniform plasticization of the red core-forming PHBMA block at 65 °C that occur on heating an aqueous dispersion of PEG_{45}−$PHBMA_{20}$ spheres. These subtle changes account for the observed sphere-to-worm and worm-to-vesicle transitions, respectively.

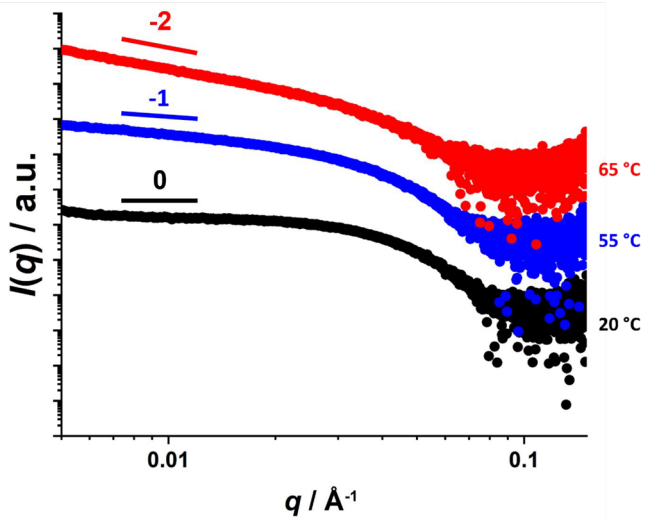

Figure 9. Representative double-logarithmic $I(q)$ vs q SAXS patterns recorded for a 1.0% w/w aqueous dispersion of thermoresponsive PEG_{45}−$PHBMA_{20}$ nano-objects prepared at 30% w/w solids at 20 °C (black), 55 °C (blue) and 65 °C (red). The characteristic low q gradients expected for spheres, worms and vesicles (0, −1, and −2, respectively) are included as a guide for the eye.

achieved within 1 h, and efficient extension of the PEG_{45}-TTC precursor with HBMA was confirmed by GPC analysis. Heating a transparent free-flowing 10% w/w dispersion of PEG_{45}−$PHBMA_{20}$ nano-objects up to 50 °C resulted in a sol−gel transition, which indicated the formation of a worm phase. At 65 °C, this dispersion became opaque and free-flowing, which suggested a worm-to-vesicle transition. After drying a 0.1% w/w aqueous dispersion of PEG_{45}−$PHBMA_{20}$ nano-objects at 25, 55, 65 or 75 °C, TEM studies confirmed the presence of spheres, worms, vesicles or lamellae, respectively. Variable temperature DLS studies confirmed that these morphological transitions are thermoreversible at copolymer concentrations as low as 0.1% w/w. Oscillatory rheology studies of a 10% w/w aqueous dispersion of these PEG_{45}−$PHBMA_{20}$ nano-objects as a function of temperature indicated a critical gelation temperature (CGT) of ∼52 °C, and the complex viscosity $|\eta^*|$ attained its maximum value at 58 °C. Furthermore, the morphological transitions for these shape-shifting nano-objects exhibited minimal hysteresis. As expected, SIPLI studies confirmed the presence of isotropic nano-objects at ambient temperature, the formation of highly anisotropic nano-objects at around 58 °C, and the re-emergence of isotropic nano-objects on further heating. Moreover, this technique indicated that anisotropic character is regained at 75 °C, as expected for a lamellar phase. Variable temperature ^{1}H NMR spectroscopy studies indicated that the sphere-to-worm and worm-to-vesicle transitions are driven by (partial) dehydration of the PEG stabilizer chains rather than by (partial) hydration of the hydrophobic PHBMA chains. However, a greater (partial) degree of hydration of the PHBMA chains was observed above 65 °C, which is consistent with the higher solvent volume fraction within the corresponding nano-objects indicated by SAXS analysis. Consideration of the fractional packing parameter suggests that the associated vesicle-to-lamellae transition must occur by a uniform plasticization mechanism, which is similar to the thermoresponsive behavior reported for PHBA-based nano-objects.[46,58,59] As far as we are aware, this is the first example of any thermoresponsive diblock copolymer nano-objects prepared via RAFT aqueous emulsion polymerization. Moreover, this particular PEG_{45}−$PHBMA_{20}$ diblock copolymer exhibits three thermoreversible transitions in aqueous solution. No doubt such behavior is related to the relatively short DP targeted for the hydrophobic PHBMA block. Moreover, the aqueous solubility of HBMA is relatively high, which suggests that the PHBMA block cannot be strongly hydrophobic. Clearly, further studies are warranted to examine whether similar thermoresponsive behavior can be achieved when targeting higher DPs for the PEG stabilizer and PHBMA blocks, respectively. However, it seems highly unlikely that such thermoresponsive behavior could ever be observed for more hydrophobic water-immiscible monomers such as styrene or benzyl methacrylate.

■ ASSOCIATED CONTENT

Supporting Information

The Supporting Information is available free of charge at https://pubs.acs.org/doi/10.1021/acs.macromol.2c00379.

^{1}H NMR spectrum recorded for PEG_{45}−$PHBMA_{20}$ diblock copolymer; DMF GPC curves recorded for both the PEG_{45}-TTC precursor and PEG_{45}−$PHBMA_{20}$ diblock copolymer; variable-temperature rheology data obtained for a 10% w/w aqueous dispersion of PEG_{45}−$PHBMA_{20}$; SIPLI obtained for a 10% w/w aqueous dispersion of PEG_{45}−$PHBMA_{20}$ at 25, 60, 63, and 70 °C; schematic cartoon showing the difference in mean core cross-sectional radius for a sphere and cylinder of the same core volume; plot of SAXS patterns for a 1.0% w/w aqueous dispersion of PEG_{45}−$PHBMA_{20}$ nano-objects prepared at 10% w/w recorded between 20 and 70 °C; SAXS patterns for a 1.0% w/w aqueous

https://doi.org/10.1021/acs.macromol.2c00379
Macromolecules 2022, 55, 3051−3062

dispersion of PEG_{45}−$PHBMA_{20}$ nano-objects prepared at 30% w/w recorded at 20, 55, and 65 °C; full experimental details of all syntheses and characterization methods; details of the three scattering models used for SAXS analysis (PDF)

AUTHOR INFORMATION

Corresponding Author

Steven P. Armes − *Dainton Building, Department of Chemistry, University of Sheffield, Sheffield, Yorkshire S3 7HF, U.K.;* orcid.org/0000-0002-8289-6351; Email: s.p.armes@sheffield.ac.uk

Authors

Saul J. Hunter − *Dainton Building, Department of Chemistry, University of Sheffield, Sheffield, Yorkshire S3 7HF, U.K.;* orcid.org/0000-0002-9280-1969

Nicholas J. W. Penfold − *Dainton Building, Department of Chemistry, University of Sheffield, Sheffield, Yorkshire S3 7HF, U.K.*

Elizabeth R. Jones − *DSM Biomedical, 6167RD Geleen, The Netherlands*

Thomas Zinn − *ESRF - The European Synchrotron, 38043 Grenoble, France*

Oleksandr O. Mykhaylyk − *Dainton Building, Department of Chemistry, University of Sheffield, Sheffield, Yorkshire S3 7HF, U.K.;* orcid.org/0000-0003-4110-8328

Complete contact information is available at: https://pubs.acs.org/10.1021/acs.macromol.2c00379

Notes

The authors declare no competing financial interest.

ACKNOWLEDGMENTS

EPSRC is thanked for a CDT PhD studentship to support S.J.H. (EP/L016281) and also an Established Career Particle Technology Fellowship (EP/R003009) for S.P.A. DSM Research (Geleen, The Netherlands) is acknowledged for partial support of this PhD project and for permission to publish this work. The authors thank Christopher Hill and Dr. Svetomir Tzokov at the University of Sheffield Biomedical Science Electron Microscopy suite. Dr. Khalid I. A. Doudin is thanked for recording the variable temperature ^{1}H NMR spectra. We also thank the ESRF (Grenoble, France) for synchrotron beamtime (proposals SC4985 and SC5109).

REFERENCES

(1) Blanazs, A.; Armes, S. P.; Ryan, A. J. Self-Assembled Block Copolymer Aggregates: From Micelles to Vesicles and their Biological Applications. *Macromol. Rapid Commun.* **2009**, *30*, 267−277.

(2) Charleux, B.; Delaittre, G.; Rieger, J.; D'Agosto, F. Polymerization-Induced Self-Assembly: From Soluble Macromolecules to Block Copolymer Nano-Objects in One Step. *Macromolecules* **2012**, *45*, 6753−6765.

(3) Warren, N. J.; Armes, S. P. Polymerization-Induced Self-Assembly of Block Copolymer Nano-objects via RAFT Aqueous Dispersion Polymerization. *J. Am. Chem. Soc.* **2014**, *136*, 10174−10185.

(4) Zetterlund, P. B.; Thickett, S. C.; Perrier, S.; Bourgeat-Lami, E.; Lansalot, M. Controlled/Living Radical Polymerization in Dispersed Systems: An Update. *Chem. Rev.* **2015**, *115*, 9745−9800.

(5) Rieger, J. Guidelines for the Synthesis of Block Copolymer Particles of Various Morphologies by RAFT Dispersion Polymerization. *Macromol. Rapid Commun.* **2015**, *36*, 1458−1471.

(6) Lowe, A. B. RAFT alcoholic dispersion polymerization with polymerization-induced self-assembly. *Polymer* **2016**, *106*, 161−181.

(7) Derry, M. J.; Fielding, L. A.; Armes, S. P. Polymerization-induced self-assembly of block copolymer nanoparticles via RAFT non-aqueous dispersion polymerization. *Prog. Polym. Sci.* **2016**, *52*, 1−18.

(8) Canning, S. L.; Smith, G. N.; Armes, S. P. A Critical Appraisal of RAFT-Mediated Polymerization-Induced Self-Assembly. *Macromolecules* **2016**, *49*, 1985−2001.

(9) Yeow, J.; Boyer, C. Photoinitiated Polymerization-Induced Self-Assembly (Photo-PISA): New Insights and Opportunities. *Advanced Science* **2017**, *4*, 1700137.

(10) Penfold, N. J. W.; Yeow, J.; Boyer, C.; Armes, S. P. Emerging Trends in Polymerization-Induced Self-Assembly. *ACS Macro Lett.* **2019**, *8*, 1029−1054.

(11) Khor, S. Y.; Quinn, J. F.; Whittaker, M. R.; Truong, N. P.; Davis, T. P. Controlling Nanomaterial Size and Shape for Biomedical Applications via Polymerization-Induced Self-Assembly. *Macromol. Rapid Commun.* **2019**, *40*, 1800438.

(12) Zhang, W. J.; Hong, C. Y.; Pan, C. Y. Polymerization-Induced Self-Assembly of Functionalized Block Copolymer Nanoparticles and Their Application in Drug Delivery. *Macromol. Rapid Commun.* **2019**, *40*, 1800279.

(13) Le, D.; Keller, D.; Delaittre, G. Reactive and Functional Nanoobjects by Polymerization-Induced Self-Assembly. *Macromol. Rapid Commun.* **2019**, *40*, 1800551.

(14) D'Agosto, F.; Rieger, J.; Lansalot, M. RAFT-Mediated Polymerization-Induced Self-Assembly. *Angew. Chem. Int. Ed* **2020**, *59*, 8368−8392.

(15) Liu, C.; Hong, C. Y.; Pan, C. Y. Polymerization techniques in polymerization-induced self-assembly (PISA). *Polym. Chem.* **2020**, *11*, 3673−3689.

(16) An, Z.; Tang, W.; Hawker, C. J.; Stucky, G. D. One-Step Microwave Preparation of Well-Defined and Functionalized Polymeric Nanoparticles. *J. Am. Chem. Soc.* **2006**, *128*, 15054−15055.

(17) An, Z.; Shi, Q.; Tang, W.; Tsung, C.-K.; Hawker, C. J.; Stucky, G. D. Facile RAFT Precipitation Polymerization for the Microwave-Assisted Synthesis of Well-Defined, Double Hydrophilic Block Copolymers and Nanostructured Hydrogels. *J. Am. Chem. Soc.* **2007**, *129*, 14493−14499.

(18) Wan, W.-M.; Hong, C.-Y.; Pan, C.-Y. One-pot synthesis of nanomaterials via RAFT polymerization induced self-assembly and morphology transition. *Chem. Commun.* **2009**, 5883−5885.

(19) Wan, W.-M.; Sun, X.-L.; Pan, C.-Y. Formation of Vesicular Morphologies via Polymerization Induced Self-Assembly and Re-Organization. *Macromol. Rapid Commun.* **2010**, *31*, 399−404.

(20) Boissé, S.; Rieger, J.; Belal, K.; Di-Cicco, A.; Beaunier, P.; Li, M.-H.; Charleux, B. Amphiphilic block copolymer nano-fibers via RAFT-mediated polymerization in aqueous dispersed system. *Chem. Commun.* **2010**, *46*, 1950−1952.

(21) Sugihara, S.; Armes, S. P.; Blanazs, A.; Lewis, A. L. Non-spherical morphologies from cross-linked biomimetic diblock copolymers using RAFT aqueous dispersion polymerization. *Soft Matter* **2011**, *7*, 10787−10793.

(22) Blanazs, A.; Madsen, J.; Battaglia, G.; Ryan, A. J.; Armes, S. P. Mechanistic Insights for Block Copolymer Morphologies: How Do Worms Form Vesicles? *J. Am. Chem. Soc.* **2011**, *133*, 16581−16587.

(23) Huang, C.-Q.; Pan, C.-Y. Direct preparation of vesicles from one-pot RAFT dispersion polymerization. *Polymer* **2010**, *51*, 5115−5121.

(24) Houillot, L.; Bui, C.; Save, M.; Charleux, B.; Farcet, C.; Moire, C.; Raust, J.-A.; Rodriguez, I. Synthesis of Well-Defined Polyacrylate Particle Dispersions in Organic Medium Using Simultaneous RAFT Polymerization and Self-Assembly of Block Copolymers. A Strong Influence of the Selected Thiocarbonylthio Chain Transfer Agent. *Macromolecules* **2007**, *40*, 6500−6509.

(25) Fielding, L. A.; Derry, M. J.; Ladmiral, V.; Rosselgong, J.; Rodrigues, A. M.; Ratcliffe, L. P. D.; Sugihara, S.; Armes, S. P. RAFT dispersion polymerization in non-polar solvents: facile production of

block copolymer spheres, worms and vesicles in n-alkanes. *Chem. Sci.* **2013**, *4*, 2081−2087.
(26) Rymaruk, M. J.; Hunter, S. J.; O'Brien, C. T.; Brown, S. L.; Williams, C. N.; Armes, S. P. RAFT Dispersion Polymerization in Silicone Oil. *Macromolecules* **2019**, *52*, 2822−2832.
(27) Blanazs, A.; Ryan, A. J.; Armes, S. P. Predictive Phase Diagrams for RAFT Aqueous Dispersion Polymerization: Effect of Block Copolymer Composition, Molecular Weight, and Copolymer Concentration. *Macromolecules* **2012**, *45*, 5099−5107.
(28) Warren, N. J.; Mykhaylyk, O. O.; Mahmood, D.; Ryan, A. J.; Armes, S. P. RAFT Aqueous Dispersion Polymerization Yields Poly(ethylene glycol)-Based Diblock Copolymer Nano-Objects with Predictable Single Phase Morphologies. *J. Am. Chem. Soc.* **2014**, *136*, 1023−1033.
(29) Liu, G.; Qiu, Q.; Shen, W.; An, Z. Aqueous Dispersion Polymerization of 2-Methoxyethyl Acrylate for the Synthesis of Biocompatible Nanoparticles Using a Hydrophilic RAFT Polymer and a Redox Initiator. *Macromolecules* **2011**, *44*, 5237−5245.
(30) Shen, W.; Chang, Y.; Liu, G.; Wang, H.; Cao, A.; An, Z. Biocompatible, Antifouling, and Thermosensitive Core−Shell Nanogels Synthesized by RAFT Aqueous Dispersion Polymerization. *Macromolecules* **2011**, *44*, 2524−2530.
(31) Liu, G.; Qiu, Q.; An, Z. Development of thermosensitive copolymers of poly(2-methoxyethyl acrylate-co-poly(ethylene glycol) methyl ether acrylate) and their nanogels synthesized by RAFT dispersion polymerization in water. *Polym. Chem.* **2012**, *3*, 504−513.
(32) Tan, J.; Sun, H.; Yu, M.; Sumerlin, B. S.; Zhang, L. Photo-PISA: Shedding Light on Polymerization-Induced Self-Assembly. *ACS Macro Lett.* **2015**, *4*, 1249−1253.
(33) Tan, J.; Bai, Y.; Zhang, X.; Huang, C.; Liu, D.; Zhang, L. Low-Temperature Synthesis of Thermoresponsive Diblock Copolymer Nano-Objects via Aqueous Photoinitiated Polymerization-Induced Self-Assembly (Photo-PISA) using Thermoresponsive Macro-RAFT Agents. *Macromol. Rapid Commun.* **2016**, *37*, 1434−1440.
(34) Tan, J.; Zhang, X.; Liu, D.; Bai, Y.; Huang, C.; Li, X.; Zhang, L. Facile Preparation of CO_2-Responsive Polymer Nano-Objects via Aqueous Photoinitiated Polymerization-Induced Self-Assembly (Photo-PISA). *Macromol. Rapid Commun.* **2017**, *38*, 1600508.
(35) Foster, J. C.; Varlas, S.; Couturaud, B.; Jones, J. R.; Keogh, R.; Mathers, R. T.; O'Reilly, R. K. Predicting Monomers for Use in Polymerization-Induced Self-Assembly. *Angew. Chem. Int. Ed* **2018**, *57*, 15733−15737.
(36) Lovell, P. A.; Schork, F. J. Fundamentals of Emulsion Polymerization. *Biomacromolecules* **2020**, *21*, 4396−4441.
(37) Zhou, J.; Yao, H.; Ma, J. Recent advances in RAFT-mediated surfactant-free emulsion polymerization. *Polym. Chem.* **2018**, *9*, 2532−2561.
(38) Ferguson, C. J.; Hughes, R. J.; Nguyen, D.; Pham, B. T. T.; Gilbert, R. G.; Serelis, A. K.; Such, C. H.; Hawkett, B. S. Ab Initio Emulsion Polymerization by RAFT-Controlled Self-Assembly. *Macromolecules* **2005**, *38*, 2191−2204.
(39) Blanazs, A.; Verber, R.; Mykhaylyk, O. O.; Ryan, A. J.; Heath, J. Z.; Douglas, C. W. I.; Armes, S. P. Sterilizable Gels from Thermoresponsive Block Copolymer Worms. *J. Am. Chem. Soc.* **2012**, *134*, 9741−9748.
(40) Lowe, A. B.; McCormick, C. L. Reversible addition−fragmentation chain transfer (RAFT) radical polymerization and the synthesis of water-soluble (co)polymers under homogeneous conditions in organic and aqueous media. *Prog. Polym. Sci.* **2007**, *32*, 283−351.
(41) Rieger, J.; Grazon, C.; Charleux, B.; Alaimo, D.; Jérôme, C. Pegylated thermally responsive block copolymer micelles and nanogels via in situ RAFT aqueous dispersion polymerization. *J. Polym. Sci., Part A: Polym. Chem.* **2009**, *47*, 2373−2390.
(42) Figg, C. A.; Simula, A.; Gebre, K. A.; Tucker, B. S.; Haddleton, D. M.; Sumerlin, B. S. Polymerization-induced thermal self-assembly (PITSA). *Chem. Sci.* **2015**, *6*, 1230−1236.
(43) Wang, X.; Zhou, J.; Lv, X.; Zhang, B.; An, Z. Temperature-Induced Morphological Transitions of Poly(dimethylacrylamide)−Poly(diacetone acrylamide) Block Copolymer Lamellae Synthesized via Aqueous Polymerization-Induced Self-Assembly. *Macromolecules* **2017**, *50*, 7222−7232.
(44) Ma, Y.; Gao, P.; Ding, Y.; Huang, L.; Wang, L.; Lu, X.; Cai, Y. Visible Light Initiated Thermoresponsive Aqueous Dispersion Polymerization-Induced Self-Assembly. *Macromolecules* **2019**, *52*, 1033−1041.
(45) Ratcliffe, L. P. D.; Derry, M. J.; Ianiro, A.; Tuinier, R.; Armes, S. P. A Single Thermoresponsive Diblock Copolymer Can Form Spheres, Worms or Vesicles in Aqueous Solution. *Angew. Chem. Int. Ed* **2019**, *58*, 18964−18970.
(46) Byard, S. J.; O'Brien, C. T.; Derry, M. J.; Williams, M.; Mykhaylyk, O. O.; Blanazs, A.; Armes, S. P. Unique aqueous self-assembly behavior of a thermoresponsive diblock copolymer. *Chem. Sci.* **2020**, *11*, 396−402.
(47) Chiefari, J.; Chong, Y. K.; Ercole, F.; Krstina, J.; Jeffery, J.; Le, T. P. T.; Mayadunne, R. T. A.; Meijs, G. F.; Moad, C. L.; Moad, G.; Rizzardo, E.; Thang, S. H. Living Free-Radical Polymerization by Reversible Addition−Fragmentation Chain Transfer: The RAFT Process. *Macromolecules* **1998**, *31*, 5559−5562.
(48) Moad, G.; Rizzardo, E.; Thang, S. H. Living Radical Polymerization by the RAFT ProcessA First Update. *Aust. J. Chem.* **2006**, *59*, 669−692.
(49) Moad, G.; Rizzardo, E.; Thang, S. H. Living Radical Polymerization by the RAFT Process − A Second Update. *Aust. J. Chem.* **2009**, *62*, 1402−1472.
(50) Moad, G.; Rizzardo, E.; Thang, S. H. Living Radical Polymerization by the RAFT Process − A Third Update. *Aust. J. Chem.* **2012**, *65*, 985−1076.
(51) Gibson, R. R.; Armes, S. P.; Musa, O. M.; Fernyhough, A. End-group ionisation enables the use of poly(N-(2-methacryloyloxy)ethyl pyrrolidone) as an electrosteric stabiliser block for polymerisation-induced self-assembly in aqueous media. *Polym. Chem.* **2019**, *10*, 1312−1323.
(52) Zhou, D.; Dong, S.; Kuchel, R. P.; Perrier, S.; Zetterlund, P. B. Polymerization induced self-assembly: tuning of morphology using ionic strength and pH. *Polym. Chem.* **2017**, *8*, 3082−3089.
(53) North, S. M.; Armes, S. P. Aqueous solution behavior of stimulus-responsive poly(methacrylic acid)-poly(2-hydroxypropyl methacrylate) diblock copolymer nanoparticles. *Polym. Chem.* **2020**, *11*, 2147−2156.
(54) Beattie, D. L.; Mykhaylyk, O. O.; Ryan, A. J.; Armes, S. P. Rational synthesis of novel biocompatible thermoresponsive block copolymer worm gels. *Soft Matter* **2021**, *17*, 5602−5612.
(55) Ratcliffe, L. P. D.; Blanazs, A.; Williams, C. N.; Brown, S. L.; Armes, S. P. RAFT polymerization of hydroxy-functional methacrylic monomers under heterogeneous conditions: effect of varying the core-forming block. *Polym. Chem.* **2014**, *5*, 3643−3655.
(56) Israelachvili, J. N.; Mitchell, D. J.; Ninham, B. W. Theory of self-assembly of hydrocarbon amphiphiles into micelles and bilayers. *J. Chem. Soc., Trans* **1976**, *72*, 1525−1568.
(57) Antonietti, M.; Förster, S. Vesicles and Liposomes: A Self-Assembly Principle Beyond Lipids. *Adv. Mater.* **2003**, *15*, 1323−1333.
(58) Deane, O. J.; Jennings, J.; Neal, T. J.; Musa, O. M.; Fernyhough, A.; Armes, S. P. Synthesis and Aqueous Solution Properties of Shape-Shifting Stimulus-Responsive Diblock Copolymer Nano-Objects. *Chem. Mater.* **2021**, *33*, 7767−7779.
(59) Deane, O. J.; Jennings, J.; Armes, S. P. Shape-shifting thermoreversible diblock copolymer nano-objects via RAFT aqueous dispersion polymerization of 4-hydroxybutyl acrylate. *Chemical Science* **2021**, *12*, 13719−13729.
(60) Cumming, J. M.; Deane, O. J.; Armes, S. P. Reversible Addition-Fragmentation Chain Transfer Aqueous Dispersion Polymerization of 4-Hydroxybutyl Acrylate Produces Highly Thermoresponsive Diblock Copolymer Nano-Objects. *Macromolecules* **2022**, *55*, 788−798.
(61) Beattie, D. L.; Deane, O. J.; Mykhaylyk, O. O.; Armes, S. P. RAFT aqueous dispersion polymerization of 4-hydroxybutyl acrylate: effect of end-group ionization on the formation and colloidal stability

https://doi.org/10.1021/acs.macromol.2c00379
Macromolecules 2022, 55, 3051−3062

of sterically-stabilized diblock copolymer nanoparticles. *Polym. Chem.* **2022**, *13*, 655−667.
(62) Wilson, S. J. Synthesis and Characterisation of Stimulus-responsive Diblock Copolymer Nano-objects Prepared by RAFT Aqueous Dispersion Polymerisation. PhD Thesis, University of Sheffield, Sheffield, UK, 2019.
(63) Romero-Azogil, L.; Penfold, N. J. W.; Armes, S. P. Tuning the hydroxyl functionality of block copolymer worm gels modulates their thermoresponsive behavior. *Polym. Chem.* **2020**, *11*, 5040−5050.
(64) Penfold, N. J. W.; Whatley, J. R.; Armes, S. P. Thermoreversible Block Copolymer Worm Gels Using Binary Mixtures of PEG Stabilizer Blocks. *Macromolecules* **2019**, *52*, 1653−1662.
(65) Warren, N. J.; Derry, M. J.; Mykhaylyk, O. O.; Lovett, J. R.; Ratcliffe, L. P. D.; Ladmiral, V.; Blanazs, A.; Fielding, L. A.; Armes, S. P. Critical Dependence of Molecular Weight on Thermoresponsive Behavior of Diblock Copolymer Worm Gels in Aqueous Solution. *Macromolecules* **2018**, *51*, 8357−8371.
(66) Cunningham, V. J.; Ratcliffe, L. P. D.; Blanazs, A.; Warren, N. J.; Smith, A. J.; Mykhaylyk, O. O.; Armes, S. P. Tuning the critical gelation temperature of thermo-responsive diblock copolymer worm gels. *Polym. Chem.* **2014**, *5*, 6307−6317.
(67) Verber, R.; Blanazs, A.; Armes, S. P. Rheological studies of thermo-responsive diblock copolymer worm gels. *Soft Matter* **2012**, *8*, 9915−9922.
(68) Zhang, W.; D'Agosto, F.; Boyron, O.; Rieger, J.; Charleux, B. One-Pot Synthesis of Poly(methacrylic acid-co-poly(ethylene oxide) methyl ether methacrylate)-b-polystyrene Amphiphilic Block Copolymers and Their Self-Assemblies in Water via RAFT-Mediated Radical Emulsion Polymerization. A Kinetic Study. *Macromolecules* **2011**, *44*, 7584−7593.
(69) Boissé, S.; Rieger, J.; Pembouong, G.; Beaunier, P.; Charleux, B. Influence of the stirring speed and CaCl2 concentration on the nano-object morphologies obtained via RAFT-mediated aqueous emulsion polymerization in the presence of a water-soluble macroRAFT agent. *J. Polym. Sci., Part A: Polym. Chem.* **2011**, *49*, 3346−3354.
(70) Zhang, W.; D'Agosto, F.; Boyron, O.; Rieger, J.; Charleux, B. Toward a Better Understanding of the Parameters that Lead to the Formation of Nonspherical Polystyrene Particles via RAFT-Mediated One-Pot Aqueous Emulsion Polymerization. *Macromolecules* **2012**, *45*, 4075−4084.
(71) Poon, C. K.; Tang, O.; Chen, X.-M.; Pham, B. T. T.; Gody, G.; Pollock, C. A.; Hawkett, B. S.; Perrier, S. Preparation of Inert Polystyrene Latex Particles as MicroRNA Delivery Vectors by Surfactant-Free RAFT Emulsion Polymerization. *Biomacromolecules* **2016**, *17*, 965−973.
(72) Lesage de la Haye, J.; Zhang, X.; Chaduc, I.; Brunel, F.; Lansalot, M.; D'Agosto, F. The Effect of Hydrophile Topology in RAFT-Mediated Polymerization-Induced Self-Assembly. *Angew. Chem. Int. Ed* **2016**, *55*, 3739−3743.
(73) Deane, O. J.; Musa, O. M.; Fernyhough, A.; Armes, S. P. Synthesis and Characterization of Waterborne Pyrrolidone-Functional Diblock Copolymer Nanoparticles Prepared via Surfactant-free RAFT Emulsion Polymerization. *Macromolecules* **2020**, *53*, 1422−1434.
(74) Truong, N. P.; Dussert, M. V.; Whittaker, M. R.; Quinn, J. F.; Davis, T. P. Rapid synthesis of ultrahigh molecular weight and low polydispersity polystyrene diblock copolymers by RAFT-mediated emulsion polymerization. *Polym. Chem.* **2015**, *6*, 3865−3874.
(75) Rieger, J.; Osterwinter, G.; Bui, C.; Stoffelbach, F.; Charleux, B. Surfactant-Free Controlled/Living Radical Emulsion (Co)-polymerization of n-Butyl Acrylate and Methyl Methacrylate via RAFT Using Amphiphilic Poly(ethylene oxide)-Based Trithiocarbonate Chain Transfer Agents. *Macromolecules* **2009**, *42*, 5518−5525.
(76) Zhang, W.; D'Agosto, F.; Dugas, P.-Y.; Rieger, J.; Charleux, B. RAFT-mediated one-pot aqueous emulsion polymerization of methyl methacrylate in the presence ofpoly(methacrylic acid-co-poly-(ethylene oxide) methacrylate) trithiocarbonate macromolecular chain transfer agent. *Polymer* **2013**, *54*, 2011−2019.
(77) Chan, D. H.; Millet, A.; Fisher, C. R.; Price, M. C.; Burchell, M. J.; Armes, S. P. Synthesis and Characterization of Polypyrrole-Coated Anthracene Microparticles: A New Synthetic Mimic for Polyaromatic Hydrocarbon-Based Cosmic Dust. *ACS Appl. Mater. Interfaces* **2021**, *13*, 3175−3185.
(78) Cunningham, V. J.; Alswieleh, A. M.; Thompson, K. L.; Williams, M.; Leggett, G. J.; Armes, S. P.; Musa, O. M. Poly(glycerol monomethacrylate)−Poly(benzyl methacrylate) Diblock Copolymer Nanoparticles via RAFT Emulsion Polymerization: Synthesis, Characterization, and Interfacial Activity. *Macromolecules* **2014**, *47*, 5613−5623.
(79) Cockram, A. A.; Bradley, R. D.; Lynch, S. A.; Fleming, P. C. D.; Williams, N. S. J.; Murray, M. W.; Emmett, S. N.; Armes, S. P. Optimization of the high-throughput synthesis of multiblock copolymer nanoparticles in aqueous media via polymerization-induced self-assembly. *React. Chem. Eng.* **2018**, *3*, 645−657.
(80) Chenal, M.; Bouteiller, L.; Rieger, J. Ab initio RAFT emulsion polymerization of butyl acrylate mediated by poly(acrylic acid) trithiocarbonate. *Polym. Chem.* **2013**, *4*, 752−762.
(81) Canning, S. L.; Cunningham, V. J.; Ratcliffe, L. P. D.; Armes, S. P. Phenyl acrylate is a versatile monomer for the synthesis of acrylic diblock copolymer nano-objects via polymerization-induced self-assembly. *Polym. Chem.* **2017**, *8*, 4811−4821.
(82) Bernard, J.; Save, M.; Arathoon, B.; Charleux, B. Preparation of a xanthate-terminated dextran by click chemistry: Application to the synthesis of polysaccharide-coated nanoparticles via surfactant-free ab initio emulsion polymerization of vinyl acetate. *J. Polym. Sci., Part A: Polym. Chem.* **2008**, *46*, 2845−2857.
(83) Binauld, S.; Delafresnaye, L.; Charleux, B.; D'Agosto, F.; Lansalot, M. Emulsion Polymerization of Vinyl Acetate in the Presence of Different Hydrophilic Polymers Obtained by RAFT/MADIX. *Macromolecules* **2014**, *47*, 3461−3472.
(84) Etchenausia, L.; Khoukh, A.; Deniau Lejeune, E.; Save, M. RAFT/MADIX emulsion copolymerization of vinyl acetate and N-vinylcaprolactam: towards waterborne physically crosslinked thermoresponsive particles. *Polym. Chem.* **2017**, *8*, 2244−2256.
(85) Galanopoulo, P.; Dugas, P.-Y.; Lansalot, M.; D'Agosto, F. Poly(ethylene glycol)-b-poly(vinyl acetate) block copolymer particles with various morphologies via RAFT/MADIX aqueous emulsion PISA. *Polym. Chem.* **2020**, *11*, 3922−3930.
(86) Akpinar, B.; Fielding, L. A.; Cunningham, V. J.; Ning, Y.; Mykhaylyk, O. O.; Fowler, P. W.; Armes, S. P. Determining the Effective Density and Stabilizer Layer Thickness of Sterically Stabilized Nanoparticles. *Macromolecules* **2016**, *49*, 5160−5171.
(87) Rymaruk, M. J.; Thompson, K. L.; Derry, M. J.; Warren, N. J.; Ratcliffe, L. P. D.; Williams, C. N.; Brown, S. L.; Armes, S. P. Bespoke contrast-matched diblock copolymer nanoparticles enable the rational design of highly transparent Pickering double emulsions. *Nanoscale* **2016**, *8*, 14497−14506.
(88) Thompson, K. L.; Cinotti, N.; Jones, E. R.; Mable, C. J.; Fowler, P. W.; Armes, S. P. Bespoke Diblock Copolymer Nanoparticles Enable the Production of Relatively Stable Oil-in-Water Pickering Nanoemulsions. *Langmuir* **2017**, *33*, 12616−12623.
(89) Chan, D. H. H.; Kynaston, E. L.; Lindsay, C.; Taylor, P.; Armes, S. P. Block Copolymer Nanoparticles are Effective Dispersants for Micrometer-Sized Organic Crystalline Particles. *ACS Appl. Mater. Interfaces* **2021**, *13*, 30235−30243.
(90) Pham, B. T. T.; Nguyen, D.; Huynh, V. T.; Pan, E. H.; Shirodkar-Robinson, B.; Carey, M.; Serelis, A. K.; Warr, G. G.; Davey, T.; Such, C. H.; Hawkett, B. S. Aqueous Polymeric Hollow Particles as an Opacifier by Emulsion Polymerization Using Macro-RAFT Amphiphiles. *Langmuir* **2018**, *34*, 4255−4263.
(91) Nguyen, D.; Huynh, V.; Pham, N.; Pham, B.; Serelis, A.; Davey, T.; Such, C.; Hawkett, B. SPION-Decorated Nanofibers by RAFT-Mediated Free Radical Emulsion Polymerization-Induced Self Assembly. *Macromol. Rapid Commun.* **2019**, *40*, 1800402.
(92) Tan, J.; Dai, X.; Zhang, Y.; Yu, L.; Sun, H.; Zhang, L. Photoinitiated Polymerization-Induced Self-Assembly via Visible Light-Induced RAFT-Mediated Emulsion Polymerization. *ACS Macro Lett.* **2019**, *8*, 205−212.

https://doi.org/10.1021/acs.macromol.2c00379
Macromolecules 2022, 55, 3051−3062

(93) Dai, X.; Yu, L.; Zhang, Y.; Zhang, L.; Tan, J. Polymerization-Induced Self-Assembly via RAFT-Mediated Emulsion Polymerization of Methacrylic Monomers. *Macromolecules* **2019**, *52*, 7468−7476.
(94) Cao, J.; Tan, Y.; Chen, Y.; Zhang, L.; Tan, J. How the Reactive End Group of Macro-RAFT Agent Affects RAFT-Mediated Emulsion Polymerization-Induced Self-Assembly. *Macromol. Rapid Commun.* **2021**, *42*, 2100333.
(95) Hatton, F. L.; Lovett, J. R.; Armes, S. P. Synthesis of well-defined epoxy-functional spherical nanoparticles by RAFT aqueous emulsion polymerization. *Polym. Chem.* **2017**, *8*, 4856−4868.
(96) Hatton, F. L.; Park, A. M.; Zhang, Y.; Fuchs, G. D.; Ober, C. K.; Armes, S. P. Aqueous one-pot synthesis of epoxy-functional diblock copolymer worms from a single monomer: new anisotropic scaffolds for potential charge storage applications. *Polym. Chem.* **2019**, *10*, 194−200.
(97) Hatton, F. L.; Derry, M. J.; Armes, S. P. Rational synthesis of epoxy-functional spheres, worms and vesicles by RAFT aqueous emulsion polymerisation of glycidyl methacrylate. *Polym. Chem.* **2020**, *11*, 6343−6355.
(98) Brotherton, E. E.; Hatton, F. L.; Cockram, A. A.; Derry, M. J.; Czajka, A.; Cornel, E. J.; Topham, P. D.; Mykhaylyk, O. O.; Armes, S. P. In Situ Small-Angle X-ray Scattering Studies During Reversible Addition−Fragmentation Chain Transfer Aqueous Emulsion Polymerization. *J. Am. Chem. Soc.* **2019**, *141*, 13664−13675.
(99) Cockram, A. A.; Neal, T. J.; Derry, M. J.; Mykhaylyk, O. O.; Williams, N. S. J.; Murray, M. W.; Emmett, S. N.; Armes, S. P. Effect of Monomer Solubility on the Evolution of Copolymer Morphology during Polymerization-Induced Self-Assembly in Aqueous Solution. *Macromolecules* **2017**, *50*, 796−802.
(100) Hunter, S. J.; Lovett, J. R.; Mykhaylyk, O. O.; Jones, E. R.; Armes, S. P. Synthesis of diblock copolymer spheres, worms and vesicles via RAFT aqueous emulsion polymerization of hydroxybutyl methacrylate. *Polym. Chem.* **2021**, *12*, 3629−3639.
(101) Bannister, I.; Billingham, N. C.; Armes, S. P.; Rannard, S. P.; Findlay, P. Development of Branching in Living Radical Copolymerization of Vinyl and Divinyl Monomers. *Macromolecules* **2006**, *39*, 7483−7492.
(102) Pei, Y.; Dharsana, N. C.; van Hensbergen, J. A.; Burford, R. P.; Roth, P. J.; Lowe, A. B. RAFT dispersion polymerization of 3-phenylpropyl methacrylate with poly[2-(dimethylamino)ethyl methacrylate] macro-CTAs in ethanol and associated thermoreversible polymorphism. *Soft Matter* **2014**, *10*, 5787−5796.
(103) Zhang, Q.; Wang, C.; Fu, M.; Wang, J.; Zhu, S. Pickering high internal phase emulsions stabilized by worm-like polymeric nanoaggregates. *Polym. Chem.* **2017**, *8*, 5474−5480.
(104) Lovett, J. R.; Derry, M. J.; Yang, P.; Hatton, F. L.; Warren, N. J.; Fowler, P. W.; Armes, S. P. Can. percolation theory explain the gelation behavior of diblock copolymer worms? *Chem. Sci.* **2018**, *9*, 7138−7144.
(105) Dorsman, I. R.; Derry, M. J.; Cunningham, V. J.; Brown, S. L.; Williams, C. N.; Armes, S. P. Tuning the vesicle-to-worm transition for thermoresponsive block copolymer vesicles prepared via polymerisation-induced self-assembly. *Polym. Chem.* **2021**, *12*, 1224−1235.
(106) Audureau, N.; Coumes, F.; Guigner, J.-M.; Nguyen, T. P. T.; Ménager, C.; Stoffelbach, F.; Rieger, J. Thermoresponsive properties of poly(acrylamide-co-acrylonitrile)-based diblock copolymers synthesized (by PISA) in water. *Polym. Chem.* **2020**, *11*, 5998−6008.
(107) He, J.; Cao, J.; Chen, Y.; Zhang, L.; Tan, J. Thermoresponsive Block Copolymer Vesicles by Visible Light-Initiated Seeded Polymerization-Induced Self-Assembly for Temperature-Regulated Enzymatic Nanoreactors. *ACS Macro Lett.* **2020**, *9*, 533−539.
(108) Pei, Y.; Sugita, O. R.; Thurairajah, L.; Lowe, A. B. Synthesis of poly(stearyl methacrylate-b-3-phenylpropyl methacrylate) nanoparticles in n-octane and associated thermoreversible polymorphism. *RSC Adv.* **2015**, *5*, 17636−17646.
(109) Fielding, L. A.; Lane, J. A.; Derry, M. J.; Mykhaylyk, O. O.; Armes, S. P. Thermo-responsive Diblock Copolymer Worm Gels in Non-polar Solvents. *J. Am. Chem. Soc.* **2014**, *136*, 5790−5798.
(110) Derry, M. J.; Mykhaylyk, O. O.; Armes, S. P. A Vesicle-to-Worm Transition Provides a New High-Temperature Oil Thickening Mechanism. *Angew. Chem.* **2017**, *129*, 1772−1776.
(111) Cumming, J. M.; Deane, O. J.; Armes, S. P. Reversible Addition-Fragmentation Chain Transfer Aqueous Dispersion Polymerization of 4-Hydroxybutyl Acrylate Produces Highly Thermoresponsive Diblock Copolymer Nano-Objects. *Macromolecules* **2022**, *55*, 788.
(112) Byard, S. J.; Williams, M.; McKenzie, B. E.; Blanazs, A.; Armes, S. P. Preparation and Cross-Linking of All-Acrylamide Diblock Copolymer Nano-Objects via Polymerization-Induced Self-Assembly in Aqueous Solution. *Macromolecules* **2017**, *50*, 1482−1493.
(113) Czajka, A.; Armes, S. P. In situ SAXS studies of a prototypical RAFT aqueous dispersion polymerization formulation: monitoring the evolution in copolymer morphology during polymerization-induced self-assembly. *Chem. Sci.* **2020**, *11*, 11443−11454.
(114) György, C.; Hunter, S. J.; Girou, C.; Derry, M. J.; Armes, S. P. Synthesis of poly(stearyl methacrylate)-poly(2-hydroxypropyl methacrylate) diblock copolymer nanoparticles via RAFT dispersion polymerization of 2-hydroxypropyl methacrylate in mineral oil. *Polym. Chem.* **2020**, *11*, 4579−4590.
(115) Mykhaylyk, O. O. Time-resolved polarized light imaging of sheared materials: application to polymer crystallization. *Soft Matter* **2010**, *6*, 4430−4440.
(116) Mykhaylyk, O. O.; Parnell, A. J.; Pryke, A.; Fairclough, J. P. A. Direct Imaging of the Orientational Dynamics of Block Copolymer Lamellar Phase Subjected to Shear Flow. *Macromolecules* **2012**, *45*, 5260−5272.
(117) Mykhaylyk, O. O.; Warren, N. J.; Parnell, A. J.; Pfeifer, G.; Laeuger, J. Applications of shear-induced polarized light imaging (SIPLI) technique for mechano-optical rheology of polymers and soft matter materials. *J. Polym. Sci., Part B: Polym. Phys.* **2016**, *54*, 2151−2170.
(118) Rymaruk, M. J.; O'Brien, C. T.; Brown, S. L.; Williams, C. N.; Armes, S. P. Effect of Core Cross-linking on the Physical Properties of Poly(dimethylsiloxane)-Based Diblock Copolymer Worms Prepared in Silicone Oil. *Macromolecules* **2019**, *52*, 6849−6860.
(119) Pedersen, J. S.; Gerstenberg, M. C. Scattering Form Factor of Block Copolymer Micelles. *Macromolecules* **1996**, *29*, 1363−1365.
(120) Pedersen, J. Form factors of block copolymer micelles with spherical, ellipsoidal and cylindrical cores. *J. Appl. Crystallogr.* **2000**, *33*, 637−640.
(121) Battaglia, G.; Ryan, A. J. Bilayers and Interdigitation in Block Copolymer Vesicles. *J. Am. Chem. Soc.* **2005**, *127*, 8757−8764.
(122) Glatter, O.; Kratky, O. *Small-Angle X-ray Scattering*; Academic Press: London, 1982.
(123) Bekiranov, S.; Bruinsma, R.; Pincus, P. Solution behavior of polyethylene oxide in water as a function of temperature and pressure. *Phys. Rev. E* **1997**, *55*, 577−585.
(124) Ashbaugh, H. S.; Paulaitis, M. E. Monomer Hydrophobicity as a Mechanism for the LCST Behavior of Poly(ethylene oxide) in Water. *Ind. Eng. Chem. Res.* **2006**, *45*, 5531−5537.
(125) Yow, H. N.; Biggs, S. Probing the stability of sterically stabilized polystyrene particles by centrifugal sedimentation. *Soft Matter* **2013**, *9*, 10031−10041.
(126) Malcolm, G.; Rowlinson, J. The thermodynamic properties of aqueous solutions of polyethylene glycol, polypropylene glycol and dioxane. *Trans. Faraday Soc.* **1957**, *53*, 921−931.
(127) Polik, W. F.; Burchard, W. Static light scattering from aqueous poly(ethylene oxide) solutions in the temperature range 20−90°C. *Macromolecules* **1983**, *16*, 978−982.
(128) Bailey, F. E.; Callard, R. Some properties of poly(ethylene oxide)1 in aqueous solution. *J. Appl. Polym. Sci.* **1959**, *1*, 56−62.
(129) Dormidontova, E. E. Role of Competitive PEO−Water and Water−Water Hydrogen Bonding in Aqueous Solution PEO Behavior. *Macromolecules* **2002**, *35*, 987−1001.
(130) Shikata, T.; Okuzono, M.; Sugimoto, N. Temperature-Dependent Hydration/Dehydration Behavior of Poly(ethylene oxide)s in Aqueous Solution. *Macromolecules* **2013**, *46*, 1956−1961.

https://doi.org/10.1021/acs.macromol.2c00379
Macromolecules 2022, 55, 3051−3062